From Infinite to Two Dimensions through the Functional Renormalization Group

C. Taranto,[1] S. Andergassen,[2] J. Bauer,[3] K. Held,[1] A. Katanin,[4] W. Metzner,[5] G. Rohringer,[1] and A. Toschi[1]

[1]*Institute for Solid State Physics, Vienna University of Technology, 1040 Vienna, Austria*
[2]*Faculty of Physics, University of Vienna, Boltzmanngasse 5, 1090 Vienna, Austria*
[3]*Department of Physics, Harvard University, 17 Oxford Street, Cambridge, Massachusetts 02138, USA*
[4]*Institute of Metal Physics, 620990 Ekaterinburg, Russia and Ural Federal University, 620002 Ekaterinburg, Russia*
[5]*Max Planck Institute for Solid State Research, 70569 Stuttgart, Germany*

We present a novel scheme for an unbiased, nonperturbative treatment of strongly correlated fermions. The proposed approach combines two of the most successful many-body methods, the dynamical mean field theory and the functional renormalization group. Physically, this allows for a systematic inclusion of nonlocal correlations via the functional renormalization group flow equations, after the local correlations are taken into account nonperturbatively by the dynamical mean field theory. To demonstrate the feasibility of the approach, we present numerical results for the two-dimensional Hubbard model at half filling.

Introduction.—Correlated electron systems display undoubtedly some of the most fascinating phenomena of condensed matter physics such as high-temperature superconductivity and quantum criticality, and with the tremendous progress to cool and control atomic gases new many-body physics is explored nowadays. These systems pose a particular challenge for theory. In this Letter, we discuss a new route for the theoretical treatment of strong correlations, which combines the strengths of two of the most successful approaches developed hitherto: dynamical mean field theory (DMFT) [1,2] and the functional renormalization group (fRG) [3–6].

DMFT represents the "quantum" extension of the classical (static) mean-field theory [2]. More formally, it provides the exact solution of a quantum many-body Hamiltonian in the limit of infinite spatial dimensions ($d \rightarrow \infty$) [1]. DMFT allows, hence, for an accurate (and nonperturbative) treatment of the local part of the correlations. Among others, it provides the essential ingredients to describe the Mott-Hubbard metal-to-insulator transition in three-dimensional bulk systems [7,8]. At the same time, the mean-field nature with respect to the spatial degrees of freedom implies that all nonlocal spatial correlations are completely neglected in DMFT.

A powerful technique to treat such nonlocal correlations is, instead, provided by the fRG. Its starting point is an exact functional flow equation [9], which yields the gradual evolution from a simple initial action to the full final action, that is, the generating functional of all one-particle irreducible vertex functions. The flow parameter (RG scale) is usually a momentum or energy cutoff. Expanding the functional flow equation yields an exact but infinite hierarchy of flow equations for the *n*-particle vertex functions, which for most calculations is truncated at the two-particle level. There have been many applications of

such weak-coupling truncations to low-dimensional fermion systems with competing instabilities and non-Fermi-liquid behavior (for a review, see [6]).

The approach we present here is coined DMF^{2}RG as the DMFT solution serves as a starting point of the fRG flow. DMF^{2}RG aims at overcoming the main restrictions of the two methods, i.e., the lack of nonlocal correlations in DMFT and the weak-coupling limitation in practical implementations of the fRG. The basic idea of the DMF^{2}RG is the following: We apply the fRG not starting from a problem without (or with trivial) correlations, but from a converged DMFT solution of the correlated system. This way, the local but possibly strong DMFT correlations, essential to capture the Mott-Hubbard physics, are fully taken into account from the very beginning. Nonlocal correlations beyond DMFT, particularly important for low-dimensional systems, will be systematically generated by the fRG flow. We note that alternative strong coupling starting points for the fRG flow were recently discussed for the Bose-Hubbard [10] and the single-impurity Anderson model [11].

Before turning to the DMF^{2}RG algorithm, let us mention alternative approaches proposed in the past to include nonlocal correlations beyond DMFT. They can be classified into cluster [12,13] and diagrammatic extensions [14–19] of DMFT. The former ones are evidently complementary in nature to DMF^{2}RG, as they provide short-range correlation beyond DMFT, but at a high numerical cost, which poses significant limits to multiband calculations. Similarly, as the diagrammatic extensions of DMFT, the DMF^{2}RG includes short- and long-range correlations on equal footing and improves the scaling with the number of orbitals. At the same time, instead of a simple selection of diagrams (e.g., second order perturbation theory, ladder, etc.), DMF^{2}RG exploits the more powerful RG and

generates parquetlike diagrammatic corrections to DMFT. This way, DMF²RG provides a systematic and unbiased treatment of electronic correlations beyond DMFT in all channels. Topologically, the same diagrams albeit with different Green's functions and vertices are obtained in the proposed parquet implementations of DΓA [14] and multi-scale methods [18,19]. This is, however, computationally much more demanding, and suffers from divergences of the two-particle irreducible vertex [19–21].

Method.—A rather flexible and effective formulation of DMF²RG (see also the Supplemental Material [22] for further details) is obtained starting from the local (or "impurity") action of DMFT,

$$S_{\text{DMFT}} = -\int_0^\beta d\tau d\tau' \sum_{i\sigma} \bar{c}_{i\sigma}(\tau)\mathcal{G}^0_{\text{AIM}}(\tau-\tau')^{-1}c_{i\sigma}(\tau') + S_{\text{int}}.$$

(1)

Here, $\bar{c}_{i\sigma}$ ($c_{i\sigma}$) are the Grassmann variables corresponding to the creation (annihilation) of a fermion with spin orientation $\sigma = \uparrow, \downarrow$ on site i, $\mathcal{G}^0_{\text{AIM}}(\tau-\tau')$ is the electronic-bath Green's function of the auxiliary effective Anderson impurity model (AIM), which in a first step needs to be determined self-consistently in DMFT [7] (see left-hand side of Fig. 1), and S_{int} is a local interaction.

With this DMFT solution as a starting point, the fRG generates a flow to the finite-dimensional action of interest

$$S_{\text{latt}} = -\int_0^\beta d\tau d\tau' \sum_{\mathbf{k}\sigma} \bar{c}_{\mathbf{k}\sigma}(\tau)G^0_{\text{latt}}(\mathbf{k},\tau-\tau')^{-1}c_{\mathbf{k}\sigma}(\tau') + S_{\text{int}},$$

(2)

where $G^0_{\text{latt}}(\mathbf{k},\tau-\tau')$ is the free propagator of the finite dimensional system, which reads $G^0_{\text{latt}}(\mathbf{k},i\omega) = (i\omega - \epsilon_{\mathbf{k}} + \mu)^{-1}$ in terms of Matsubara frequencies, the energy-momentum dispersion $\epsilon_{\mathbf{k}}$, and the chemical potential μ. In Fig. 1 the specific case of a 2D square lattice is shown.

For the DMF²RG scheme we now introduce a flow parameter Λ [25] so that $G^0_\Lambda(\mathbf{k},i\omega)^{-1} = \Lambda\mathcal{G}^0_{\text{AIM}}(i\omega)^{-1} + (1-\Lambda)G^0_{\text{latt}}(\mathbf{k},i\omega)^{-1}$ interpolates between the initial DMFT ($\Lambda_{\text{initial}} = 1$) and the final action ($\Lambda_{\text{final}} = 0$).

The flow of DMF²RG, hence, gradually switches off the DMFT bath and switches on the 2D hopping, including nonlocal correlations beyond DMFT. Neglecting three (and more) particle vertices, the flow equations [6,27] for the self-energy and the two-particle vertex are shown in Fig. 1. The truncation of the hierarchy at the level of the two-particle vertex Γ relies on the assumption that the relevant physics is captured by the structure appearing on the two-particle level. Let us emphasize, however, that three- (and more-) particle vertices are included on the local level by DMFT. This flow scheme results in the following single-scale propagator (defined as $\partial G_\Lambda/\partial\Lambda|_{\Sigma^\Lambda\text{fixed}}$),
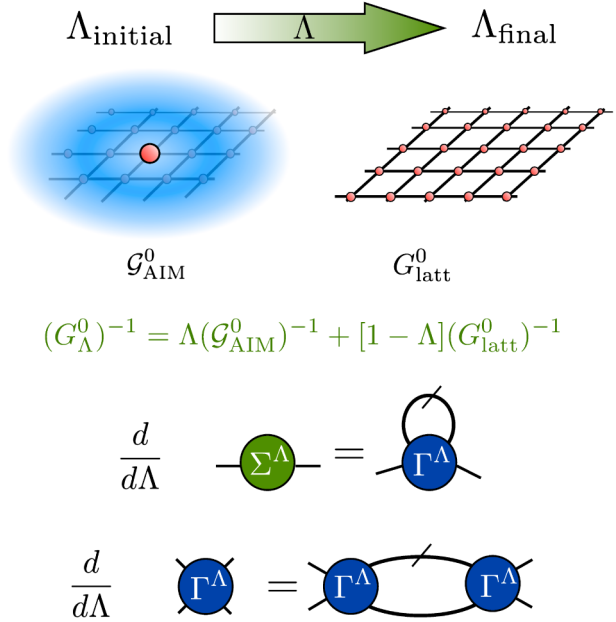

FIG. 1 (color online). Schematic illustration of the DMF²RG approach, showing the evolution of the Gaussian part G^0_Λ of the action from DMFT to its exact expression for a two-dimensional system. The (truncated) flow equations for the self-energy Σ^Λ and the two-particle vertex Γ^Λ are explicitly given in terms of Feynman diagrams.

$$S_\Lambda(\mathbf{k},i\omega) = G^2_\Lambda(\mathbf{k},i\omega)[G^0_{\text{latt}}(\mathbf{k},i\omega)^{-1} - \mathcal{G}^0_{\text{AIM}}(i\omega)^{-1}],$$

(3)

which includes the full Green's function $G_\Lambda(\mathbf{k},i\omega) = [G^0_\Lambda(\mathbf{k},i\omega)^{-1} - \Sigma^\Lambda(\mathbf{k},i\omega)]^{-1}$.

While the formal structure of the flow equations, diagrammatically depicted in Fig. 1, resembles the one of the conventional fRG implementation, in the DMF²RG the initial conditions strongly differ, as they are determined, both at the one- and the two-particle level, by DMFT, which provides the initial self-energy $\Sigma^{\Lambda=1} = \Sigma_{\text{DMFT}}(i\omega)$ and one-particle irreducible (1PI) vertex $\Gamma^{\Lambda=1} = \Gamma_{\text{DMFT}}(i\nu_1, i\nu_2; i\nu'_1, i\nu'_2)$ [28]. As a consequence, DMF²RG is numerically more expensive than the conventional fRG or DMFT schemes: (i) two-particle vertices have to be computed in DMFT [29] as an input to the 1PI-fRG flow and (ii) the frequency dependence of Σ^Λ and Γ^Λ has to be included in the fRG [32], with a proper frequency-dependent parametrization; according to a generic estimate the numerical effort scales as $N^4_k N^4_\omega$, N_k (N_ω) being the number of momenta (frequencies). DMF²RG allows us to bypass the sign problem of a direct quantum Monte Carlo (QMC) treatment of nonlocal correlations, since QMC usage will be limited, at most, to DMFT calculations of one- and two-particle local vertices.

Application to the 2D Hubbard model.—We now show, as a first application of DMF²RG, results for a prototypical model of correlated fermions, the two-dimensional Hubbard model. We recall that the interplay of

antiferromagnetism and superconductivity in this model
has been studied by weak coupling truncations of various
versions of the fRG already some time ago [33–36]. In
standard second-quantization notation, the Hubbard
Hamiltonian reads [37]

$$H = -t \sum_{\langle ij \rangle \sigma} c_{i\sigma}^{\dagger} c_{j\sigma} + U \sum_i n_{i\uparrow} n_{i\downarrow}, \qquad (4)$$

where t denotes the nearest-neighbor hopping amplitude on
a square lattice and U the local Coulomb repulsion. In the
following, we will define our energies in terms of $4t \equiv 1$,
and fix the average particle density to half filling $n = 1$. In
this case, the momentum transfer of $(\pi, \pm\pi)$ corresponds to
perfect (antiferromagnetic) nesting on the square shaped
Fermi surface.

We solve the truncated flow equations numerically,
including the self-energy feedback in the equation for
Γ^Λ. We use a channel decomposition of the interaction
vertex [22,38] with Matsubara frequency dependence of the
self-energy and the interaction vertex. The momentum-
dependence is taken into account by discretizing the
Brillouin zone into patches with momentum-independent
initial vertex function. If fine enough, this discretization
captures the angular variation of the vertex function along
the Fermi surface with good precision. For simplicity, we
restrict ourselves to 8 patches, which already includes
important physical aspects of the 2D system [39].

Numerical results.—Our calculations for the two-particle
vertex function and self-energy are reported in Figs. 2 and
3–4, respectively. In Fig. 2 we plot the largest component
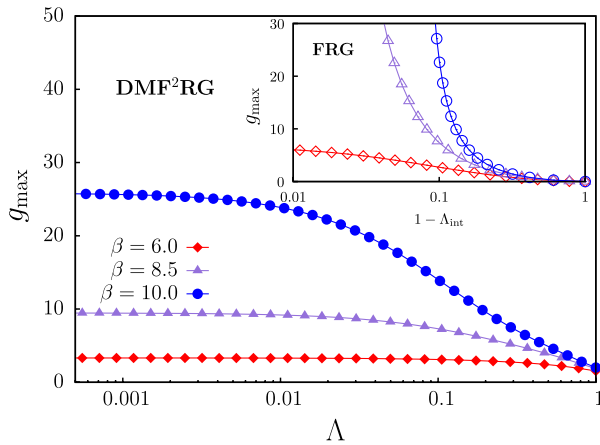(g_{max}) of the vertex function, which–at half filling–is found

in the particle-hole crossed channel for zero frequency and
antiferromagnetic momentum transfer (π, π). The data,
which refer to a weak-intermediate regime ($U = 1$), clearly
show that the DMF^{2}RG mitigates the fRG tendency to a
low-T divergence of the flow: We still obtain a converged
DMF^{2}RG result for g_{max} at $\beta = 1/T = 10$, whereas the
fRG flow for the vertex is manifestly divergent [40].
Quantitatively, by fixing an upper bound for g_{max}, we
observe that the temperature at which it is reached is
slightly decreased in DMF^{2}RG compared to fRG for
moderate values of the interaction (up to $U = 0.75$) while
is significantly decreased from $T \sim 0.125$ (fRG) to ~ 0.085
(DMF^{2}RG) at $U = 1$. This is attributed to the damping
effect of the local correlations, included from the very
beginning in the flow of DMF^{2}RG. We emphasize that this
"divergence" is *not* associated with a true onset of a long-
range order. In fact, fRG schemes can be adapted to access
also the disordered phase at lower T [41], though such an
extension goes beyond the scope of this work.

We now turn to the analysis of the self-energy results
obtained with the DMF^{2}RG flow at the lowest temperature
considered, i.e., $\beta = 10$. Here, the fRG flow diverges, and it
is worth comparing the DMF^{2}RG results with the original
DMFT data; see Fig. 3. As expected in two dimensions, the
nonlocal correlations captured by the DMF^{2}RG strongly
modify the DMFT (**k**-independent) results, determining a
significant momentum dependence of the self-energy at
low frequencies: While in DMFT, a metallic solution with a
moderate Fermi-liquid renormalization of the quasiparticle
mass is obtained; in DMF^{2}RG we observe a strong
enhancement of the imaginary part of the self-energy at

FIG. 2 (color online). Flow of the largest component (g_{max}) of
the two-particle vertex function, i.e., in our case, Γ in the particle-
hole crossed channel, for zero transfer frequency ($\nu_2 - \nu_1' = 0$),
antiferromagnetic momentum transfer [$\mathbf{k}_2 - \mathbf{k}_1' = (\pi, \pi)$] and
$\mathbf{k}_1 = (0, \pi)$, $\mathbf{k}_2 = (\pi, 0)$ computed by fRG, with interaction
cutoff Λ_{int}[26] (inset) and DMF^{2}RG (main panel) for the two-
dimensional half-filled Hubbard model at $U = 1$, at different
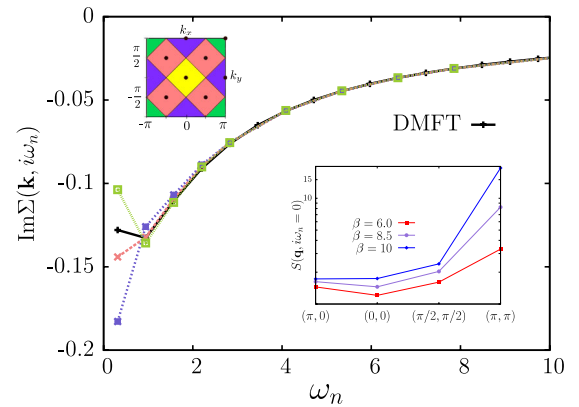(inverse) temperatures.

FIG. 3 (color online). Comparison of the results for the
imaginary part of the fermionic self-energy of the two-dimen-
sional Hubbard model for $U = 1$, and $\beta = 10$, calculated within
DMFT (**k** independent, in black) and DMF^{2}RG, for different **k**
vectors [the color coding of the different **k** is defined in the inset,
note that the values of Im$\Sigma(\mathbf{k}, i\omega_n)$ for $\mathbf{k} = (0, 0)$ and (π, π)
coincide because of the particle-hole symmetry]. Upper inset:
Scheme of the 8 patches discretization used for the calculations.
Lower inset: T dependence of the momentum-resolved static spin
susceptibility $S(\mathbf{q}, i\Omega = 0)$.

PHYSICAL REVIEW LETTERS
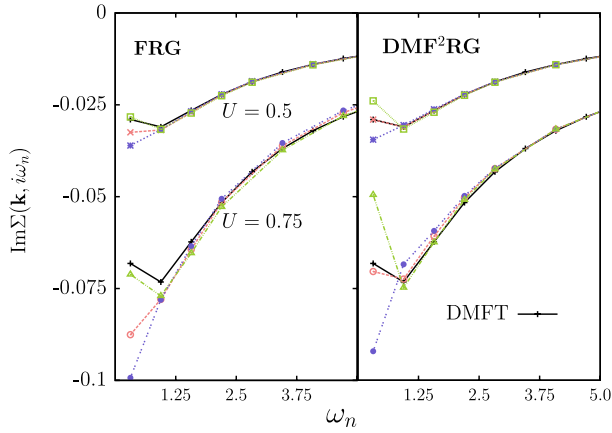
FIG. 4 (color online). Comparison of the imaginary part of the self-energy for $U = 0.5$, 0.75, $n = 1$, and $\beta = 10$, calculated by fRG and DMF^{2}RG, for different **k** vectors (color coding as in Fig. 3).

the Fermi surface. In fact, at the "antinodal" point $(\pi, 0)$, where the largest value of $-\mathrm{Im}\Sigma$ is found, the low-frequency behavior is manifestly non-quasi-particle-like, indicating the destruction of the Fermi surface in this region of the Brillouin zone. The trend of large nonlocal corrections to DMFT at the antinodal momentum and towards a pseudogap formation is similar to cluster-DMFT results [13,42]. Deviations from the DMFT metallic results, albeit less marked, are found at the "nodal" point $(\pi/2, \pi/2)$, for which one cannot exclude, at this temperature, a residual presence of strongly damped quasiparticle excitations. The significant reduction of $-\mathrm{Im}\Sigma$ with respect to DMFT, observed at $(0,0)$ or (π, π), does not imply metallicity since these points are far away from the Fermi surface, and the real part of the self-energy (not shown) is also strongly enhanced with respect to DMFT. A further insight on the nonlocal correlations captured by the DMF^{2}RG is given by the analysis of the momentum- or frequency-dependent susceptibilities, which in DMF^{2}RG can be extracted from the two-particle vertex. In the lower inset of Fig. 3, we show the DMF^{2}RG results for the momentum-resolved static spin susceptibility $S(\mathbf{q}, i\Omega = 0)$. This quantity is most important at half filling, where magnetic fluctuations predominate, and it is experimentally accessible, e.g., via neutron spectroscopy. Our results are in qualitative agreement with the QMC data of Refs. [43,44] and show the major role played by antiferromagnetic fluctuations, with a pronounced peak at (π, π), growing upon decreasing T. The ferromagnetic fluctuations also get enhanced due to the van Hove singularity at the Fermi level.

In Fig. 4, we compare the DMF^{2}RG self-energy data with the fRG. The comparison can only be performed at weaker coupling and/or higher T than in Fig. 3, as the fRG flow needs to converge. Our numerical data of Fig. 4 indicate that in the considered parameter region (same T,

but weaker interaction than in Fig. 3) the fRG and DMF^{2}RG yield qualitatively similar results for the **k**-dependent self-energy. Considering that in DMF^{2}RG local correlations have been included nonperturbatively via DMFT, this confirms the validity of previous fRG analysis of the Hubbard model at weak and moderate interaction. At the same time, the applicability of DMF^{2}RG goes beyond the weak-to-intermediate coupling of the fRG, allowing for the study of parameter regions where the Mott-Hubbard physics "already" captured by DMFT becomes important. Technically, a full treatment of this regime requires an improvement of the frequency parametrization of the 1PI vertex in the fRG flow beyond the current frequency decomposition [38].

Summary and outlook.—We introduced the DMF^{2}RG approach, which exploits the synergy of local DMFT correlations and nonlocal correlations generated by the fRG flow. Applying DMF^{2}RG to the 2D Hubbard model, we find that, due to the inclusion of all local correlations by the DMFT starting point, the divergence of the flow for the interaction vertex is pushed to lower temperatures, where significant nonlocal corrections to DMFT are found. At the same time, in the temperature interval where both fRG and DMF^{2}RG converge, the self-energy results are qualitatively similar, supporting the results of previous fRG studies at weak-to-intermediate U. Quantitatively, the most visible effect of DMF^{2}RG compared to fRG consists of a stronger **k** dependence of the self-energy for the considered parameters and a suppression of the "pseudocritical" temperature at which the vertex diverges. We emphasize, finally, the potential of the presented DMF^{2}RG approach to access the strong-coupling regime, where the Mott-Hubbard physics captured by DMFT will play a more important role and qualitative changes in the self-energy results are to be expected. The flexibility of the DMF^{2}RG scheme and its ability to avoid the sign problem of a direct QMC treatment of nonlocal physics beyond DMFT look promising for future, unbiased studies of correlations in realistic multiband models.

[1] W. Metzner and D. Vollhardt, Phys. Rev. Lett. **62**, 324 (1989).
[2] A. Georges and G. Kotliar, Phys. Rev. B **45**, 6479 (1992).

[3] M. Salmhofer, *Renormalization* (Springer, Berlin, 1999).

[4] J. Berges, N. Tetradis, and C. Wetterich, Phys. Rep. **363**, 223 (2002).

[5] P. Kopietz, L. Bartosch, and F. Schütz, *Introduction to the Functional Renormalization Group* (Springer, Berlin, 2010).

[6] W. Metzner, M. Salmhofer, C. Honerkamp, V. Meden, and K. Schönhammer, Rev. Mod. Phys. **84**, 299 (2012).

[7] A. Georges, G. Kotliar, W. Krauth, and M. Rozenberg, Rev. Mod. Phys. **68**, 13 (1996).

[8] P. Hansmann, A. Toschi, G. Sangiovanni, T. Saha-Dasgupta, S. Lupi, M. Marsi, and K. Held, Phys. Status Solidi B **250**, 1251 (2013).

[9] C. Wetterich, Phys. Lett. B **301**, 90 (1993).

[10] A. Rancon and N. Dupuis, Phys. Rev. B **83**, 172501 (2011); **84**, 174513 (2011).

[11] M. Kinza, J. Ortloff, J. Bauer, and C. Honerkamp, Phys. Rev. B **87**, 035111 (2013).

[12] M. H. Hettler, A. N. Tahvildar-Zadeh, M. Jarrell, T. Pruschke, and H. R. Krishnamurthy, Phys. Rev. B **58**, R7475 (1998); G. Kotliar, S. Y. Savrasov, G. Pálsson, and G. Biroli, Phys. Rev. Lett. **87**, 186401 (2001).

[13] T. A. Maier, M. Jarrell, T. Pruschke, and M. H. Hettler, Rev. Mod. Phys. **77**, 1027 (2005).

[14] A. Toschi, A. A. Katanin, and K. Held, Phys. Rev. B **75**, 045118 (2007); A. Valli, G. Sangiovanni, O. Gunnarsson, A. Toschi, and K. Held, Phys. Rev. Lett. **104**, 246402 (2010); G. Rohringer, A. Toschi, A. A. Katanin, and K. Held, Phys. Rev. Lett. **107**, 256402 (2011).

[15] A. N. Rubtsov, M. I. Katsnelson, and A. I. Lichtenstein, Phys. Rev. B **77**, 033101 (2008); H. Hafermann, G. Li, A. N. Rubtsov, M. I. Katsnelson, A. I. Lichtenstein, and H. Monien, Phys. Rev. Lett. **102**, 206401 (2009).

[16] G. Rohringer, A. Toschi, H. Hafermann, K. Held, V. I. Anisimov, and A. A. Katanin, Phys. Rev. B **88**, 115112 (2013).

[17] J. P. Hague, M. Jarrell, and T. C. Schulthess, Phys. Rev. B **69**, 165113 (2004).

[18] C. Slezak, M. Jarrell, Th. Maier, and J. Deisz, J. Phys. Condens. Matter **21**, 435604 (2009).

[19] S.-X. Yang, H. Fotso, H. Hafermann, K.-M. Tam, J. Moreno, T. Pruschke, and M. Jarrell, arXiv:1104.3854v1.

[20] T. Schäfer, G. Rohringer, O. Gunnarsson, S. Ciuchi, G. Sangiovanni, and A. Toschi, Phys. Rev. Lett. **110**, 246405 (2013).

[21] V. Janiš, and V. Pokorný, arXiv:1403.2507.

[22] See Supplemental Material at http://link.aps.org/supplemental/10.1103/PhysRevLett.112.196402, which includes Refs. [23,24], for further details.

[23] C. Platt, W. Hanke, and R. Thomale, Adv. Phys. **62**, 453 (2013).

[24] H. Park, K. Haule, and G. Kotliar, Phys. Rev. Lett. **107** 137007 (2011).

[25] The multiplicative cutoff is chosen in analogy to the interaction flow scheme [26], see also Supplemental Material [22].

[26] C. Honerkamp, D. Rohe, S. Andergassen, and T. Enss, Phys. Rev. B **70**, 235115 (2004).

[27] M. Salmhofer and C. Honerkamp, Prog. Theor. Phys. **105**, 1 (2001).

[28] The computation of the full dynamical structure of the local two-particle vertex of DMFT, though numerically demanding, became feasible recently. For the details about the local two-particle vertex functions of DMFT, see Refs. [14,20,29–32].

[29] G. Rohringer, A. Valli, and A. Toschi, Phys. Rev. B **86**, 125114 (2012).

[30] J. Kuneš, Phys. Rev. B **83**, 085102 (2011).

[31] H. Hafermann, arXiv:1311.5801.

[32] M. Kinza and C. Honerkamp, Phys. Rev. B **88**, 195136 (2013).

[33] D. Zanchi and H. J. Schulz, Phys. Rev. B **61**, 13609 (2000).

[34] C. J. Halboth and W. Metzner, Phys. Rev. B **61**, 7364 (2000).

[35] C. Honerkamp, M. Salmhofer, N. Furukawa, and T. M. Rice, Phys. Rev. B **63**, 035109 (2001).

[36] A. P. Kampf and A. A. Katanin, Phys. Rev. B **67**, 125104 (2003).

[37] J. Hubbard, Proc. R. Soc. A **276**, 238 (1963).

[38] C. Karrasch, R. Hedden, R. Peters, T. Pruschke, K. Schönhammer, and V. Meden, J. Phys. Condens. Matter **20**, 345205 (2008).

[39] E. Gull, M. Ferrero, O. Parcollet, A. Georges, and A. J. Millis, Phys. Rev. B **82**, 155101 (2010).

[40] We note in passing that the fRG data presented in Fig. 2 have been obtained with the interaction cutoff, but we have verified that these results are robust with respect to the choice of the cutoff.

[41] T. Baier, E. Bick, and C. Wetterich, Phys. Rev. B **70**, 125111 (2004).

[42] We note that the enhancement of the overall spread of Im$\Sigma(\mathbf{k}, i\omega_n)$ from fRG to DMF^{2}RG shows a behavior consistent with DCA calculations for increasing cluster size; O. Gunnarsson (private communication).

[43] S. R. White, D. J. Scalapino, R. L. Sugar, E. Y. Loh, J. E. Gubernatis, and R. T. Scalettar, Phys. Rev. B **40**, 506 (1989).

[44] N. E. Bickers and S. R. White, Phys. Rev. B **43**, 8044 (1991).